Environmental Earth Sciences (2024) 83:366
https://doi.org/10.1007/s12665-024-11670-7

ORIGINAL ARTICLE

Identification of deep Czech Republic–Austria transboundary aquifer discharge and associated river chloride loading

Kateřina Chroustová[1] · Adam Říčka[1] · Bibiána Pasternáková[1] · Tomáš Kuchovský[1] · Thomas R. Rüde[2] · Josef Zeman[1]

Received: 31 October 2023 / Accepted: 11 May 2024

Abstract

The deep transboundary aquifer of regional scale along the Czech Republic–Austria border in Central Europe serves as a thermal-mineral water resource for balneotherapy and plays an important role in the region's development. The aquifer is composed mostly of Jurassic carbonates at depths from 160 to − 3000 masl. Despite more than two decades of exploitation, no complex analysis of groundwater flow directions and groundwater fluxes ever took place. Now, cross-border cooperation enabled the research team to gather crucial information on the Jurassic aquifer. For a better understanding of the groundwater flow system, a numerical model was developed. To simulate the effect of variable density and viscosity occurring in such a deep aquifer, the SEAWAT numerical model was used. The simulation shows that there is an inflow of low mineralised groundwater from the crystalline outcrops in the northwest and inflow of saline groundwater from southeast. Aquifer discharge was identified along the zone partly corresponding to the course of the Dyje River. To check the model's accuracy, the river water was sampled together with streamflow measurements. Detected sections of increasing chloride concentration indicate zones of the Jurassic aquifer discharge into the Dyje River. The discharge rate of 85 L/s derived from streamflow and chloride concentrations matches the value computed by the model. The relatively high discharge of the Jurassic aquifer contributes significantly to the high chloride loading observed in the Dyje River.

Keywords Deep aquifer · Transboundary aquifer · Variable density and viscosity flow · Numerical model · Groundwater discharge · River chloride load

Introduction

Transboundary aquifers often hold large amounts of groundwater (IGRAC 2021). A transboundary aquifer is an aquifer that crosses national borders, i.e. its parts are located in different national states (IGRAC 2021).

One such aquifer lies along the Czech Republic-Austria border in Central Europe. This deep-seated sedimentary reservoir mostly composes of Jurassic carbonates (Jurassic aquifer). It covers an area of about 1400 km^2 and provides thermal-mineral water for balneology in both countries. Wells are about 1.5 km deep. Although this natural resource has been used for more than 20 years, no complex hydrogeological characterisation has taken place so far. A comprehensive understanding of the hydrogeological system is needed to protect this aquifer from overexploitation, which is a major risk for water resource sustainability (Custodio 2002).

A close cross-border collaboration enabled the research team to gather crucial information from previous research conducted in the area. The study region is abundant in hydrocarbon resources (Picha et al. 2006), which is why most of the information about the Jurassic aquifer comes from records of drilling of hydrocarbon exploratory wells. This information made it possible to draft the groundwater flow pattern of the Jurassic aquifer, which is controlled by the configuration of hydraulic heads and by the distribution of hydraulic conductivity (Sophocleous 2004). The knowledge of the groundwater flow pattern enables to derive recharge and discharge rates (Tóth 2009). However, a wide range of groundwater mineralisation and temperatures are present in such a deep aquifer affecting groundwater head

✉ Kateřina Chroustová
436416@mail.muni.cz

[1] Department of Geological Sciences, Faculty of Sciences, Masaryk Univ, Kotlarska 2, 61137 Brno, Czech Republic

[2] Hydrogeology, RWTH Aachen University, Lochnerstr 4-20, 52064 Aachen, Germany

Published online: 28 May 2024

data. Because of this, a variable-density and viscosity flow model was developed to derive groundwater flow patterns.

This type of model is commonly used to simulate seawater intrusion (Beheshti et al. 2022; Agossou et al. 2022; Chang et al. 2020), groundwater contamination (Yoon et al. 2023; Okuhata et al. 2022; Colombani et al. 2015), radioactive waste disposal (Kapyrin 2021; Malkovsky and Pek 2013), and deep aquifers consisting of both fresh and saline groundwater (Senger 1993).

The simulation of a real groundwater flux requires a thorough knowledge of the spatial distribution of hydraulic conductivity together with the observed hydraulic heads and aquifer geometry (Freeze and Witherspoon 1968). However, the sparse and predominantly archival data available on the Jurassic aquifer meant the simulated groundwater discharge was verified by hydrochemical sampling and hydrological survey of the Dyje River, which is the major drainage system in the study region. The groundwater from the Jurassic aquifer should flow upward and seep into the Dyje River. The upward flow from deep aquifers may cause the salinization of shallow aquifers and thereby influence the shallow water chemistry (Tóth 2009; Moore et al. 2009; De Louw et al. 2010; Larsen et al. 2021). For this reason, the chemical composition of the Dyje water was also carefully examined to check for the presence of deep Jurassic aquifer discharge as indicated by the numerical model.

Description of the study area

The study area is in Central Europe, in the border area between the Czech Republic and Austria (Fig. 1). Spa resorts using thermal mineral water from the aquifer are located near the Pasohlavky village approx. 30 km south from Brno (Czech Republic) and in the city of Laa an der Thaya approx. 57 km north from Vienna (Austria). The study area belongs to the Outer Western Carpathian lowlands (Bína and Demek 2012). Elevation varies from 290 m above sea level (masl) in the northwest to 170 masl in the southeast. Average annual temperatures range from 9 to 11 °C. The average annual sum of precipitation in most of the study area is between 500 and 550 mm and in the lowest parts it is below 500 mm (Chmi.cz 2023). It is one of the driest areas of the Czech Republic and Austria (Tolasz et al. 2007).

The area is drained by the Dyje river and its tributaries (Fig. 1). Though a major part of the area is used for intensive agriculture, the most significant source of pollution is the wastewater discharged into the Dyje river from the chemical factory Jungbunzlauer Austria AG producing citric acid in Pernhofen (Fig. 3). The wastewater contains high concentrations of dissolved solids, chlorides, sulphates, nitrates, and concentrations of organic substances, cyanides, and heavy metals (Cu, Zn). Additional contamination of the Dyje river comes from its tributary the Pulkava loaded by organic pollution from domestic sewage (Mlejnková et al. 2007).

Geological settings

The study region belongs to the Carpathian foredeep, in Austria known as the Molasse Zone (Brzobohatý and Cicha 1993), which is a part of Neogene basins formed in the foreland of the Outer Western Carpathians flysch nappes during the Alpine orogeny (Chlupáč et al. 2002). Neogene sediments are underlain by a crystalline Proterozoic basement and its Paleozoic and Mesozoic sedimentary cover (Krásný et al. 2012; Picha et al. 2006).

In the northwest, the area is formed by crystalline rocks of the Bohemian Massif, which continues to the southeast far below the overlying Neogene sediments (Picha et al. 2006). The overlying Mesozoic sequence begins with clastic rocks of the Middle Jurassic (Dogger) up to 1500 m thick in the southeast, followed by mostly carbonate sedimentation of the Upper Jurassic reaching a thickness of about 660 m (Picha et al. 2006; Adámek 1986). As a result of the crystalline basement decline, the Upper Jurassic sediments increase in thickness in the southeast direction (Krásný et al. 1987). Additionally, there are two facies of these sediments, a marginal-carbonatic, in the northwest represented by limestones and dolomites and a deeper basinal-pelitic-carbonatic in the southeast, which is represented by carbonates and the Mikulov Marls with a maximum thickness of about 1000 m (Adámek 1986, 2005). The transition zone between both Jurassic facies (Fig. 2) is called the Mušov Zone (Adámek 1974, 1977). Upward, the Mikulov Marls gradually transition into approximately 400 m thick Upper Jurassic Kurdějov Limestones (Picha et al. 2006; Adámek 2005). The Upper Jurassic carbonates and the crystalline rocks in the northwest of the study area are covered by Neogene sediments. The Neogene sedimentation begins with the Aquitanian (in the Austrian part of study area) and Burdigalian (in the Czech part) clastic rocks represented by gravels, sands, and clays (Krásný et al. 2012), followed by the Karpatian clayey sediments and siltstones with sandstone lenses and ends with the Langhian sands and clays (Adámek 2003; Chlupáč et al. 2002; Franzová 1986).

A NE-SW fault system occurs in the crystalline basement and overlying Jurassic and Neogene sediments (Adámek et al. 1990; Franzová 1973). The faults detected by the geophysical survey were formed as a result of thrust loading over the foreland in the Neogene (Adámek 2005).

Hydrogeological settings

Based on the geological settings, six geological units (GU) were identified (Fig. 2).

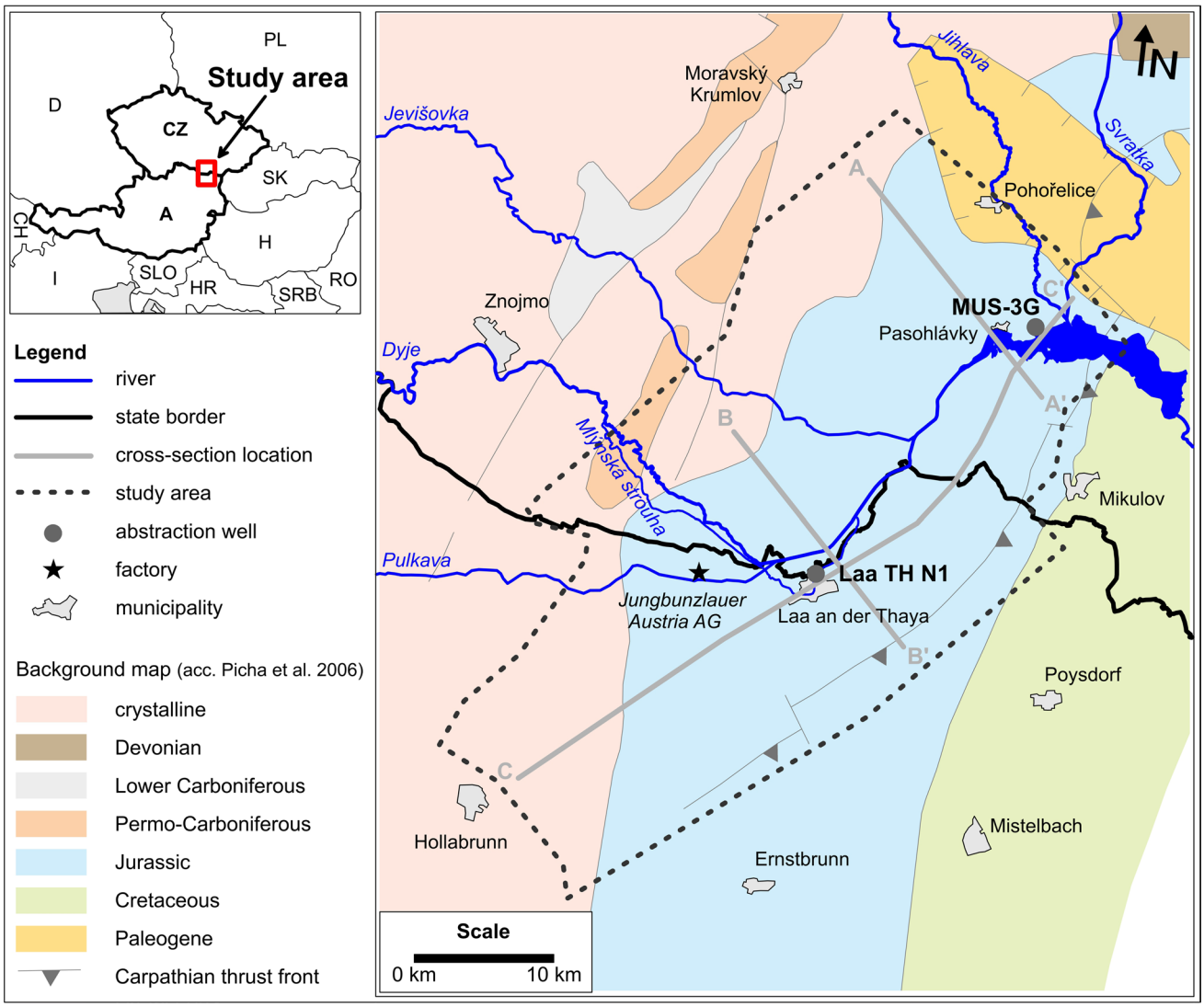

Fig. 1 Localization of the study area and deep abstraction wells MUS-3G and Laa TH N1, cross section of A-A′, B-B′ and C–C′ are shown in Fig. 2. The background map showing the basement of the Neogene sediments was modified from source Picha et al. (2006). *CZ* Czech Republic, *A* Austria, *D* Germany, *PL* Poland, *SK* Slovakia, *H* Hungary, *RO* Romania, *SRB* Serbia, *HR* Croatia, *SLO* Slovenia, *I* Italy, *CH* Switzerland

The lowest unit is the approximately 50 m thick weathered zone of crystalline rocks of the Bohemian Massif (GU1). The overlying Jurassic sediments represent the main reservoir of thermal mineral water (groundwater) and are composed of the Middle Jurassic (Dogger) clastic sediments (GU2). Above them are the Upper Jurassic carbonates (GU3). The Mikulov Marls (GU4) and the Upper Jurassic Kurdějov Limestones (Lst) (GU5) occur in the deeper southeastern part. The uppermost unit comprises the relatively permeable sediments in the Aquitanian and Burdigalian sediments (GU6).

These units form on a regional scale one aquifer. It is referred to as Jurassic aquifer as the Jurassic units are the main ones. The Jurassic aquifer is overlaid by a Neogene aquifer composed mostly of low permeable sediments (Krásný et al. 2012).

The Jurassic aquifer can be subdivided into a relatively shallow northwestern part and a deeper southeastern part separated by the Mušov Zone. The groundwater in both parts corresponds to the Na-Cl hydrochemical type. However, they differ significantly in mineralisation and temperature.

The mineralisation of the groundwater is between 0.4 and 20 g/L, with temperature ranging between 12 and 60 °C in the northwestern part of the Jurassic aquifer. The groundwater is of meteoric origin mixed with highly mineralised groundwater (Adámek et al. 1990). Topinka et al. (1992) consider this part of the aquifer as semi-open, having a natural recharge area and discharged only by pumping. The

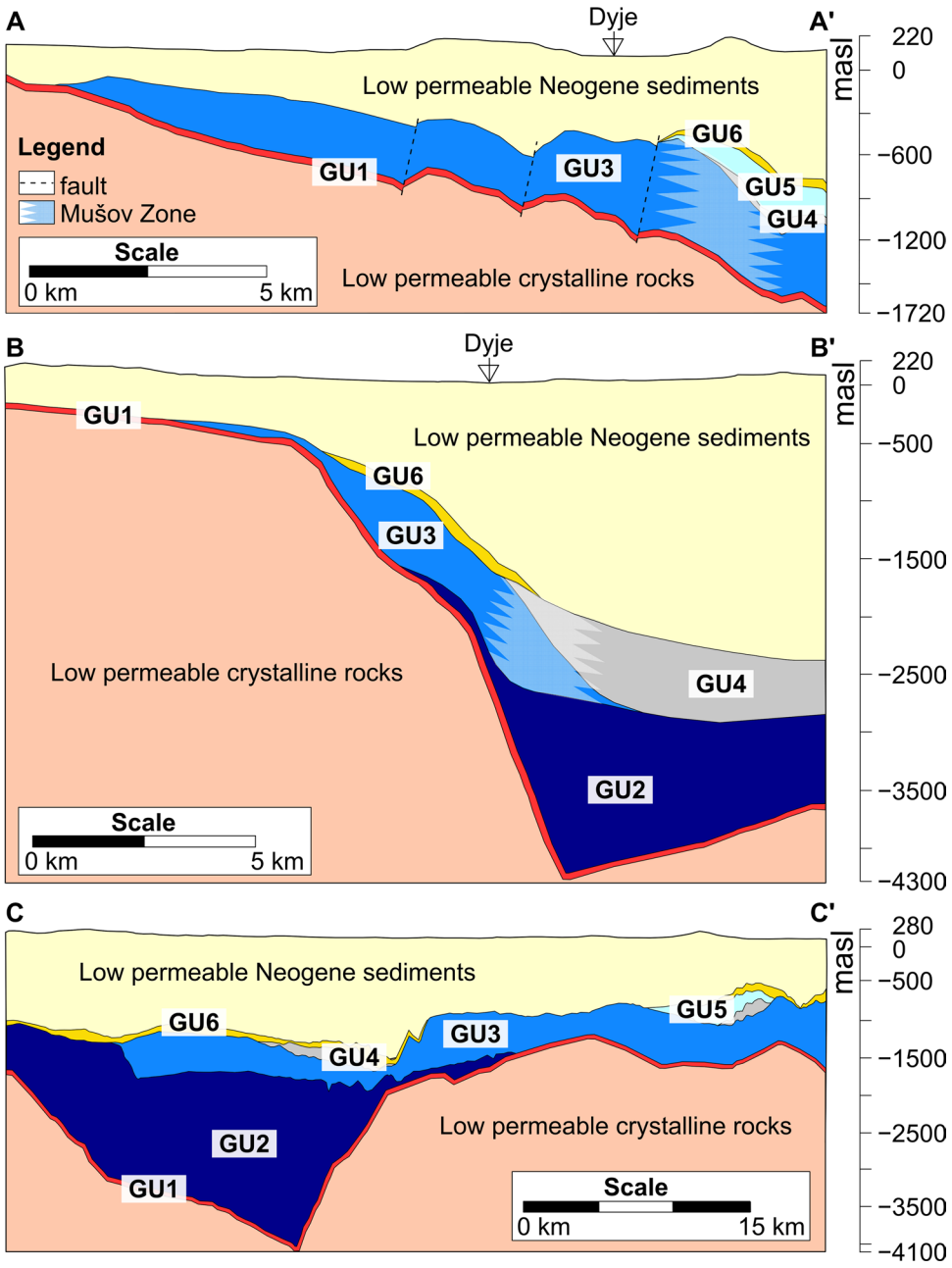

Fig. 2 Cross-sections A–A′, B–B′ and C–C′ through all six geological units (GU). Position of the Mušov Zone in cross-sections A–A′ and B–B′ according to Adámek (2005). Cross-section C–C′ was created along the Mušov Zone. Location in Fig. 1. *GU1* Crystalline rocks, *GU2* Middle Jurassic sediments, *GU3* Upper Jurassic carbonates, *GU4* Mikulov Marls, *GU5* Upper Jurassic Kurdějov Limestone, *GU6* Aquitanian and Burdigalian sediments

groundwater recharge area is assumed to be in the northwest, on the outcrops of the Bohemian Massif (Novotná and Bartoň 2011).

The northwestern part of the aquifer supplies groundwater to Czech and Austrian spa resorts for balneotherapy. The groundwater is abstracted by two deep wells (Fig. 1): Mušov 3G (MUS-3G; 1455 m deep) in Pasohlávky (Czech Republic) and Laa Thermal Nord-1 (Laa TH N1; 1448 m deep) in Laa an der Thaya (Austria) (Adámek et al. 1990; Michalíček et al. 2005).

The deeper southeastern part of the Jurassic aquifer contains saline groundwater with mineralisation ranging from 20 to 56 g/L and temperature from 60 to 136 °C. Topinka et al. (1992) describe this structure containing highly mineralised groundwater as closed without natural recharge and discharge.

According to Krásný et al. (2012) the Jurassic aquifer drainage should occur in the vicinity of the Dyje and Jevišovka river confluence (Fig. 1).

Methods

Materials and data

The hydrogeological conditions in the Jurassic aquifer were drawn upon the documentation of wells drilled within the

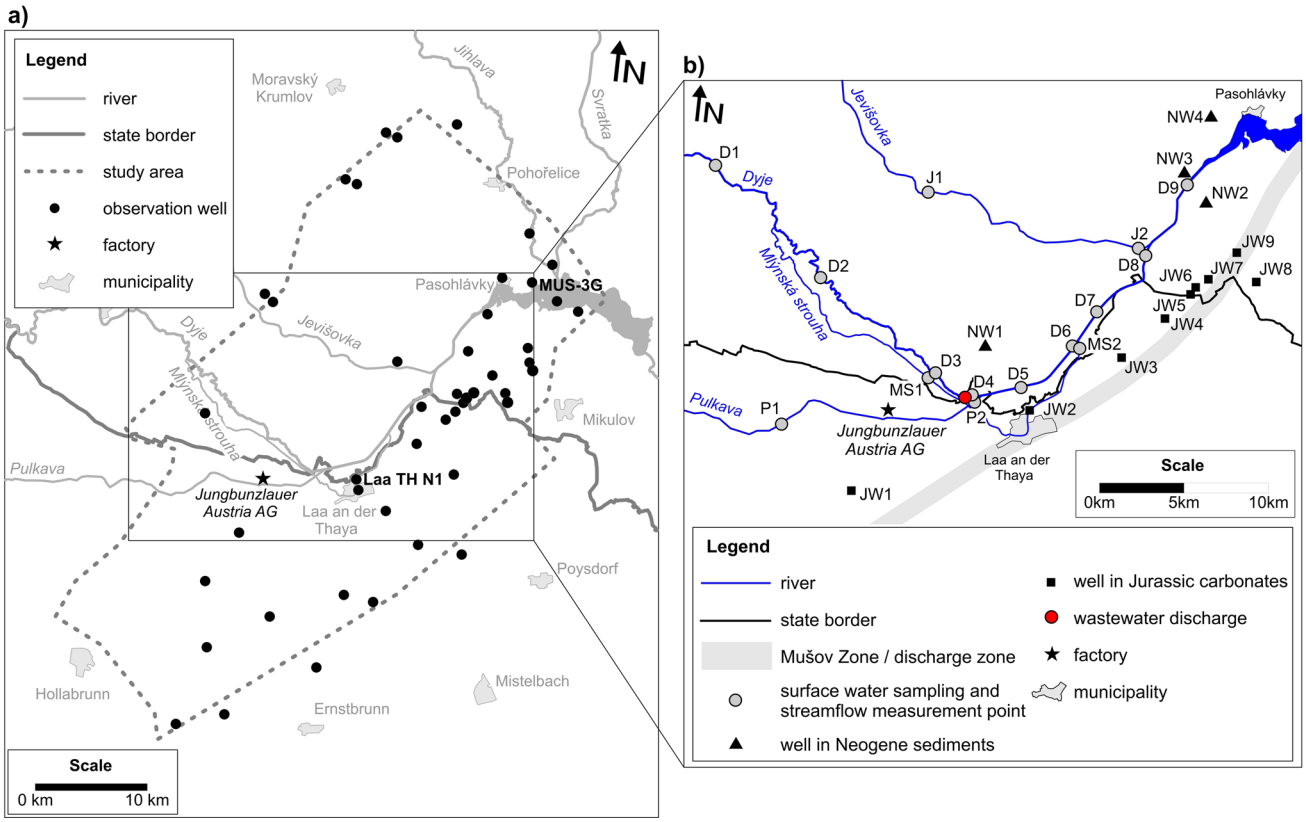

Fig. 3 **a** Location of wells reaching the Jurassic aquifer and **b** location of the water sampling and streamflow measurement points, position of the Mušov Zone according to Adámek (2005)

Czech part of the study area kept in the Czech Geological Survey archives and the company MND. Hydrogeological datasets from wells drilled in the Austrian part of the study area were provided by the Geological Survey of Austria and OMV company. The documentation includes records of aquifer tests, hydraulic conductivity values, pressure measurements, and physicochemical properties of the thermal-mineral water measured from 1950 to 1990s. The data from abstraction wells MUS-3G (Kocman 2020) and Laa TH N1 (Geological Survey of Austria) and 2 shallow wells observed by the Czech Hydrometeorological Institute comes from measurements made between 2010 and 2019. In total, 46 wells were used for the hydrogeological characterization of the Jurassic aquifer (Fig. 3a). Details on the data sources of these wells are in the Appendix 1.

Hydraulic conductivity

The spatial distribution of hydraulic conductivity was determined using the values published in archival documents and calculated from archival aquifer test data that has not been evaluated yet. The archival documents provided hydraulic conductivities obtained from 23 pumping tests and laboratory permeability tests on 21 core samples. Records of 10 pumping and recovery tests were analysed using the Cooper-Jacob straight-line method (Cooper and Jacob 1946). Furthermore, 8 values of hydraulic conductivity were calculated using steady-state pumping tests evaluated according to Thiem (1906). The radius of influence for the pumping well was estimated using the Sichardt formula (Kyrieleis and Sichardt 1930).

Hydraulic heads

Significant differences in pressure, mineralisation, and temperature causing variation in the density of groundwater had to be considered when deriving an accurate groundwater flow pattern in the Jurassic aquifer.

The correction for density variations, based on the conversion of 27 observed hydraulic heads to the hydraulic heads in groundwater with the uniform density (fresh water heads), was applied using Eq. (1) as derived by Post et al. (2007).

$$h_{f,i} = \frac{\rho_i}{\rho_f} h_i - \frac{\rho_i - \rho_f}{\rho_f} z_i \quad (1)$$

where $h_{f,i}$ is fresh water head (m), ρ_i is water density at measurement point i (kg/m^3) calculated by the software PanSystem Version 5.2 (Weatherford), ρ_f is fresh water density (kg/m^3), h_i is point water head (m) and z_i is the mean level of the well screen (m).

In order to derive the groundwater flow directions, the fresh water heads need to be calculated at the same reference depth z_r (m), i.e. corresponding fresh water heads $h_{f,r}$ (m) according to Eq. (2) as derived by Post et al. (2007).

$$h_{f,r} = z_r + \frac{\rho_i}{\rho_f}\left(h_i - z_i\right) - \frac{\rho_a}{\rho_f}\left(z_r - z_i\right) \quad (2)$$

where ρ_a is the average water density (kg/m^3) between the screens (z_i and z_r level).

Numerical flow model

The extent of the GU was identified using well-log data and a geophysical survey combined with the available lithological description of the boreholes. A 3D model of the GU forming the Jurassic aquifer and a spatial distribution model of groundwater mineralisation and temperature were constructed using the program Groundwater Modeling System Version 10.5 (Aquaveo). Programs included in this Graphic User Interface were used to develop 3D variable-density flow model.

The regional groundwater flow in the Jurassic aquifer was simulated using the equivalent porous media approach (Scanlon et al. 2003). The groundwater flow model was created with the computer program MODFLOW-2000 (Harbaugh et al. 2000). Transport model created in MT3DMS (Zheng and Wang 1999) and MODFLOW were coupled in SEAWAT program (Langevin et al. 2008) to develop a 3D model of variable-density flow. The groundwater flow model accounted for fluid viscosity variations as well, due to the wide temperature range in the aquifer. The input and resulting data were interpolated by the inverse-distance weighting method.

Water sampling and streamflow measurements

To verify the Jurassic aquifer's discharge into the Dyje river, a field survey involving water sampling and streamflow measurements was conducted on 4 May 2022. Fifteen samples were collected from the Dyje and its main tributaries the Pulkava, Mlýnská strouha, and Jevišovka (Fig. 3b). To get a better idea about groundwater composition in the overlying Neogene aquifer, 4 groundwater samples from wells (NW1, NW2, NW3, NW4) located near the Dyje river were taken (Fig. 3b). The depth of these wells ranged from 60 to 450 m, and the sampling was made under pumping conditions. All the water samples were stored after filtering (0.45 µm) in plastic bottles at 4 °C until analysis. Major cation and anion concentrations were analysed at the Department of Geological Sciences, Masaryk University in Brno. The concentrations of Mg^{2+}, K^+, and Na^+ were analysed by Atomic Absorption Spectroscopy (AAS). Concentrations of Ca^{2+}, HCO_3^-, Cl^- were analysed by titration, SO_4^{2-} and NO_3^- by the gravimetric method and sodium salicylate method, respectively. The charge balance error of all samples is less than 5% (calculated by Geochemist's Workbench 12.0).

Streamflow measurements were made using the OTT C2 current meter (counter Z400). Some streamflow measurement profiles coincide with gauging stations of the Czech Hydrometeorological institute (D1, D7, J1). Measured streamflow rates match accurately the values reported by Czech Hydrometeorological Institute, which states an uncertainty of streamflow measurement of 5%.

Results and discussion

Conceptual model

Based on the combination of geological and hydrogeological data describing the studied aquifer, the conceptual model was developed.

Aquifer extent and hydraulic conductivity

The study part of the Jurassic aquifer is restricted by the slopes of the Bohemian Massif in the northwest and by a line through the Mikulov and Ernstbrunn cities (Fig. 3a). The top and bottom of the Jurassic aquifer occurs at depths from 160 to − 3000 masl and 110 to − 4400 masl, respectively. Figure 4 shows the 3D hydrogeological model and cross-sections of the Jurassic aquifer in close vicinity of the abstraction wells.

The aquifer was divided into 6 GU to capture this spatial heterogeneity adequately. The hydraulic conductivity values specified within each GU are summarized in the Table 1. The values range from 4.2×10^{-10} m/s in GU4 to 6.0×10^{-4} m/s in GU3. The highest hydraulic conductivity was observed in the relatively shallow northwestern part.

Groundwater flow directions

The hydraulic heads observed in groundwater of variable density were converted to fresh water heads in groundwater with a uniform density of 1000 kg/m^3. These fresh water heads are represented by a map of hydraulic heads isolines (Fig. 5) based on observation at 27 deep wells.

When tracing groundwater flow directions, the fresh water heads should be evaluated at the reference level

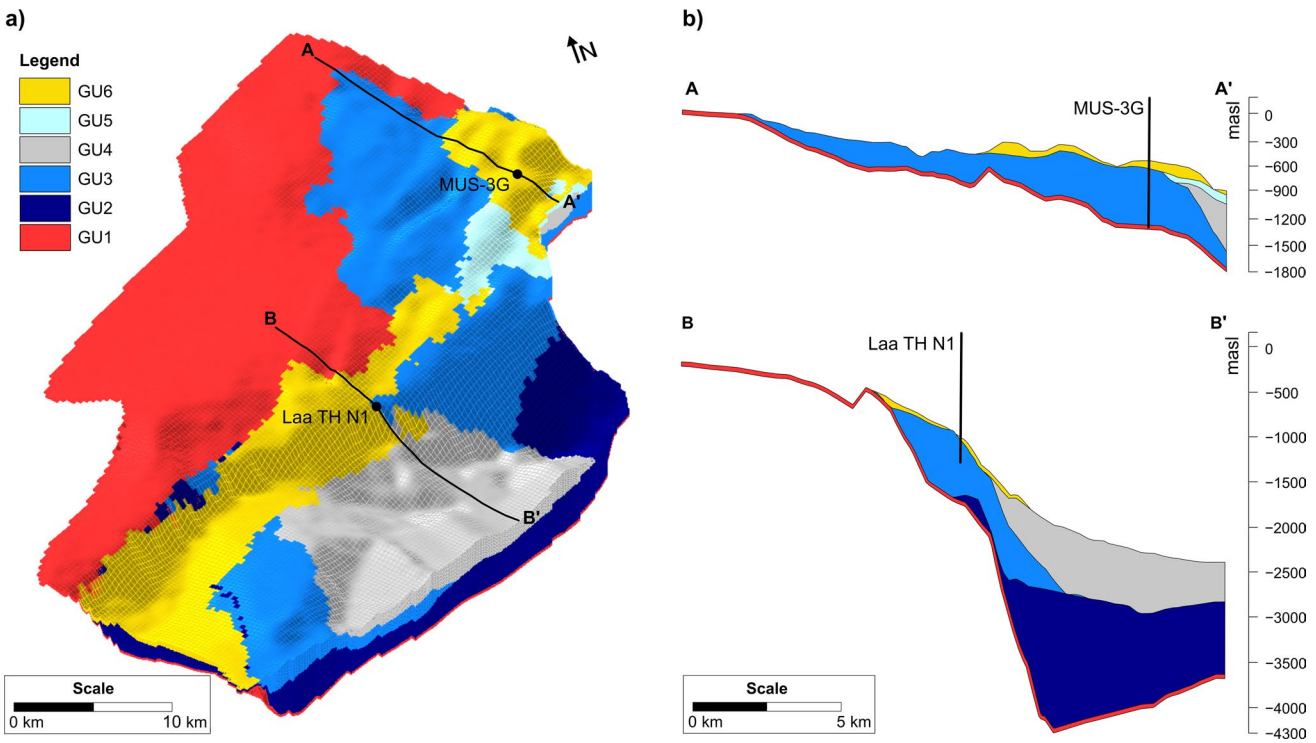

Fig. 4 **a** 3D hydrogeological model (exceeded 3 times) and cross-sections A-A′ and **b** B-B′ in the area of abstractions wells MUS-3G and Laa TH N1

Table 1 Statistical characteristic of hydraulic conductivity (HC) values within the investigated geological units (GU)

GU	Description	HC					Number of HC values		
		Min	Max	Geometric mean	Median	Standard deviation	Derived	Published (archives)	
		[m/s]	[m/s]	[m/s]	[m/s]	[m/s]	Aquifer tests	Laboratory testing	Pumping tests
GU6	Egerian and Eggenburgian sediments	1.6E–07	2.3E–05	8.9E–07	9.8E–07	6.0E–06	3	9	1
GU5	Upper Jurassic Kurdějov Lst	1.6E–07	2.2E–06	4.9E–07	4.8E–07	5.7E–07	1	11	0
GU4	Mikulov Marls	–	–	–	4.2E–10[a]	–	0	0	0
GU3	Upper Jurassic carbonates	1.3E–09	6.0E–04	5.5E–07	8.2E–07	1.3E–04	11	1	9
GU2	Middle Jurassic sediments	6.9E–09	6.4E–05	4.1E–07	2.7E–07	1.6E–05	2	0	13
GU1	Crystalline rocks	–	–	–	1.2E–08	–	1	0	0

[a]Value derived by model calibration

because hydraulic heads in groundwater of variable density will also vary with depth under the hydrostatic conditions (Post et al. 2007). Consequently, the estimate of average water density between well screens and the reference level must be defined to calculate the corresponding fresh water head (Eq. 2). However, the determination of average density can be a significant source of uncertainty in the resulting hydraulic heads (Post et al. 2007), especially in a tilted Jurassic aquifer of a regional scale. For this reason, only approximate groundwater flow directions were estimated in this study (Fig. 5).

The highest levels of fresh water head, close to 221 and 265 masl, were found along northwestern and southeastern border of the study region. The lowest fresh water heads having 190

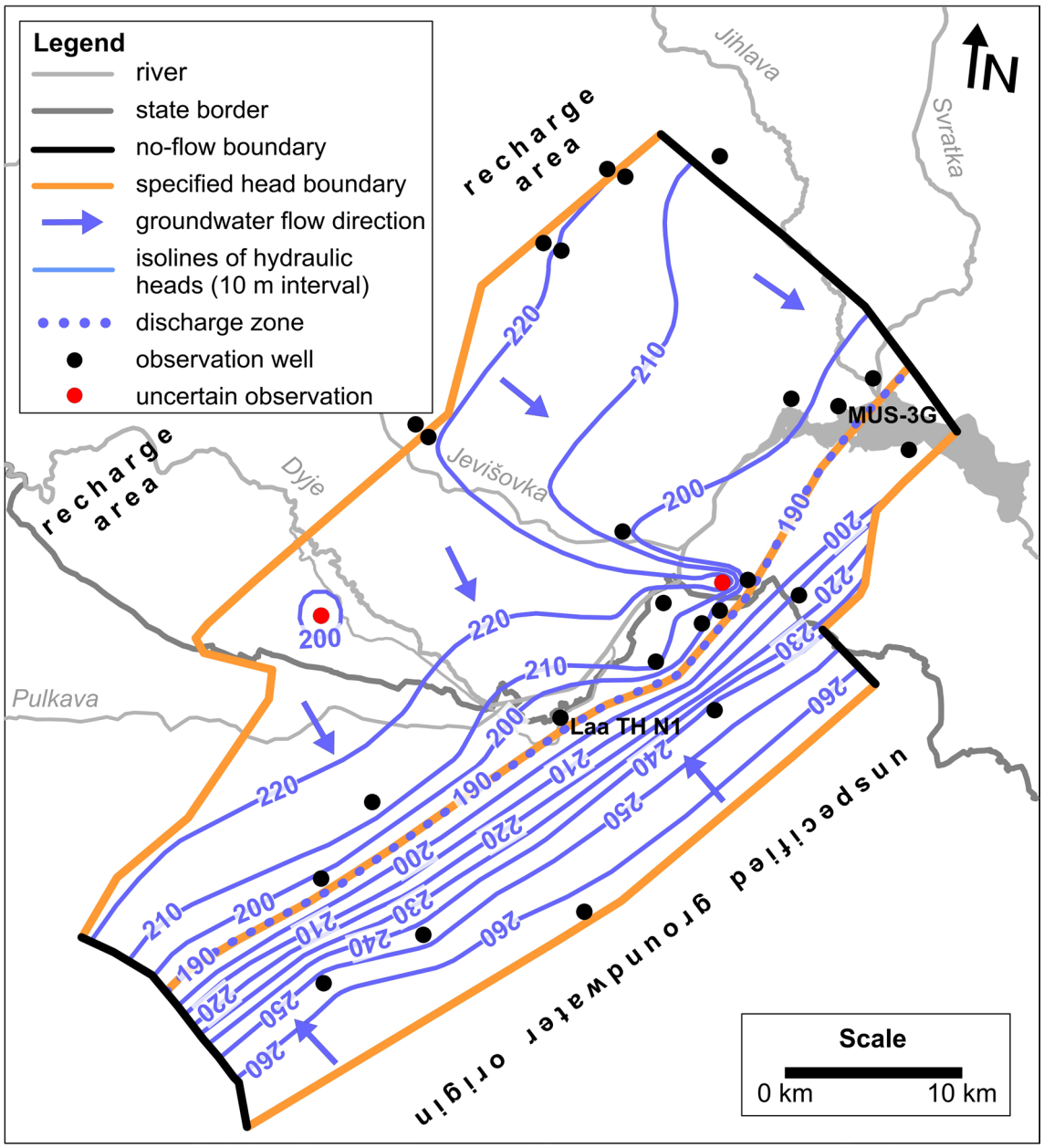

Fig. 5 Conceptual model of the studied part of Jurassic aquifer

masl were located along the Mušov Zone passing approximately through the centre of the study region in a NE/SW direction (Fig. 5). The general groundwater flow direction is in the southeastern part from SE to NW and in the northeastern part from NW to SE towards the discharge zone identified along the Mušov Zone. The northeastern part of the discharge zone is parallel to the course of the Dyje river (Fig. 5). The surface water table in the Dyje river ranges from 181 to 171 masl, thus an upward flow of groundwater from the confined Jurassic aquifer into the Dyje river can be expected there. The groundwater recharge area of this aquifer is situated in the northwest, outside of the modelled area. The groundwater origin from the southeast is unspecified.

The groundwater flow directions are subject to uncertainty associated with the average groundwater density. For this reason, a numerical model was developed to reflect the groundwater variable density and specify the initial assessment of groundwater flow directions and flux.

Numerical model

Boundary conditions and model grid

The model, covering the study part of the Jurassic aquifer, is bounded by specific head boundaries along northwestern and southeastern perimeter. The northeastern and southwestern perimeter of the model are characterized by a no-flow boundary condition, representing the contact of the Jurassic aquifer with low permeable rocks in the northeast and a streamline in the southwest. Groundwater discharge occurs along the Mušov Zone. This zone is simulated by specified head boundary located in the uppermost model layer, where the Jurassic aquifer discharges into the overlying sediments.

The modelled area was divided into a grid of 116 rows and 194 columns forming cells with a uniform horizontal size of 300 × 300 m. The model grid consists of 50 layers that capture the slope of the aquifer. The model grid is oriented along the NW–SE direction, which corresponds to the general flow direction of the groundwater.

Input parameters

To simulate the transport the hydrodynamic dispersion coefficient, molecular diffusion and effective porosity were defined. The value of longitudinal dispersivity 10 m was used according to Xu et al. (2015). Dispersivity corresponding to horizontal transverse and horizontal vertical dispersivity was multiplied by factor 0.1 and 0.01. Molecular diffusion coefficient of mineralization and temperature was set according to Langevin et al. (2008) to 1.74×10^{-14} m^2/s and 1.86×10^{-6} m^2/s, respectively. Porosity values determined by laboratory testing of rock samples from well cores are listed in Table 2. 3D model of mineralisation (Online Appendix 2a) and temperature (Online Appendix 2b) was developed by interpolation of observed values. Totally 120 observations of groundwater mineralisation and 91 observations of temperature at 34 deep wells were used. This spatial distribution was used MT3DMS. The transport time was set to short time only to create data sets required for SEAWAT.

The variable density of groundwater in the confined Jurassic aquifer was simulated under the steady-state flow conditions. The initial simulations were made with the median values of hydraulic conductivity within each GU (Table 1) with the ratio of horizontal to vertical hydraulic conductivity being 10 as the default setting.

The effect of variable water density and viscosity on groundwater flow was simulated using the variable density and viscosity packages that are included in SEAWAT program. The minimum density value was set to 930 kg/m^3 and the maximum density to 1050 kg/m^3. The reference fluid density was 1000 kg/m^3. The dependence of fluid density on pressure was expressed by the approximate value of 0.00446 (kg/m^3)/m, as per Langevin et al. (2008). The dynamic viscosity values were calculated with the PanSystem program (Weatherford) and ranges from 2.42×10^{-4} to 7.25×10^{-4} kg/(m·s). The reference dynamic viscosity value of 8.904×10^{-4} kg/(m·s) was set as suggested by Langevin et al. (2008). The full set of parameters and their values used in the SEAWAT calculation is in Table 3.

Model calibration

To ensure the model is able to adequately simulate real groundwater flow through the Jurassic aquifer, it was calibrated using the fresh water heads observed in the 22 wells inside the area (27 observations are available in total, but three wells are located outside the modelled area and two observed hydraulic heads appear to be uncertain, see Fig. 5).

After initial trial-and-error calibration that improved the boundary condition settings and approximated hydraulic conductivity to an acceptable level, the model was calibrated using the automatic calibration with the PEST code. To determine the spatial distribution of hydraulic conductivity that yields an optimal correspondence between observed and simulated hydraulic heads, the highly parametrized optimization was used (Doherty and Hunt 2010). The model domain's spatial parameterization was achieved within zones formed by GU. Each GU was assigned a network of pilot points representing locations where hydraulic conductivity was estimated. At wells where aquifer test data

Table 2 Porosity values assigned to each geological unit (GU)

GU	Description	Porosity %
GU6	Egerian and Eggenburgian sediments	18.6
GU5	Upper Jurassic Kurdějov Lst	4.7
GU4	Mikulov Marls	1.0
GU3	Upper Jurassic carbonates	5.9
GU2	Middle Jurassic sediments	13.0
GU1	Crystalline rocks	5.5

Table 3 Parameters used in SEAWAT simulation

Parameter	Value	Unit
Minimum fluid density	930	kg/m^3
Maximum fluid density	1050	kg/m^3
Reference fluid density	1000	kg/m^3
Density/pressure slope	0.00446	(kg/m^3)/m
Minimum dynamic viscosity	0.00024	kg/(m·s)
Maximum dynamic viscosity	0.00072	kg/(m·s)
Reference dynamic viscosity	0.00089	kg/(m·s)

was available, the pilot points were assigned a fixed value of hydraulic conductivity. The adjustable range of hydraulic conductivity assigned to each pilot point corresponds to the values observed within the respective GU. To obtain more realistic distribution of hydraulic conductivities, the Tikhonov regularization was used together with SVD-Assist regularization. Acceptable level of match to the observed hydraulic heads was specified by mean of PHIMLIM (Doherty and Hunt 2010) to achieve geologically plausible calibrated parameters.

The calibration evaluation is demonstrated through residuals which portray the disparity between observed and computed hydraulic heads (Fig. 6). Residuals are distributed randomly while clustering around a diagonal line. The calibration error consists of the following statistical parameters: the mean error 0.2 m (ME), the mean absolute error 1.7 m (MAE), the root mean square error 2.2 m (RMSE), and the normalized root mean square error 3.1% (NRMSE). NRMSE eliminates the dependence of RMSE on the range of observed hydraulic heads. Both the calibrating plot and error statistics attest to the model being well calibrated. The locations of the 22 calibration wells are depicted in Fig. 7a.

Model results and uncertainty

The developed numerical model confirmed the initially indicated principal groundwater flow directions and computed the groundwater fluxes through the modelled part of the Jurassic aquifer. The distribution of simulated fresh water heads at the top layer of the model is shown in the Fig. 7a. It is evident that the northwestern, relatively shallow part of the aquifer is characterized by low hydraulic gradients, unlike the southeastern part where the gradients are steeper (Fig. 7a). The zone of relatively low hydraulic conductivity was inferred through model calibration along the fault in northwestern part near MUS-3G well. This zone (Fig. 7a) was simulated using Horizontal Flow Barrier package (Hsieh and Freckleton 1993) with assigned hydraulic characteristic 1×10^{-11} m/s. The hydrodynamic role of remaining faults is unclear due to lack of hydrogeological observations. The simulated flux of groundwater through the modelled aquifer is 350 L/s. Only about 3 L/s is exploited by MUS-3G and Laa TH N1 well in total, thus most of the groundwater is discharged through upward flow along the Mušov Zone into formation top (Fig. 7b).

The primary source of model uncertainty stems from the lack of hydraulic head observations. Moreover, the hydraulic head data used for the model's calibration were observed at different times. Most of the wells had been plugged and abandoned, making it impossible to measure the hydraulic heads again. Consequently, the only feasible way of validating the model's results is to check the simulated value of groundwater flux from the part of the Jurassic aquifer where the discharge zone is parallel to the Dyje river, which is expected to drain the groundwater discharged from the northeastern part of the Jurassic aquifer (Fig. 3b). The model suggests that approximately 80 L/s should be discharged into the Dyje river in this zone. This is why the river's hydrochemistry and streamflows were evaluated to verify the simulated value of groundwater influx from the Jurassic aquifer to the Dyje river.

Field investigation of Jurassic aquifer discharge into the Dyje river

Water chemistry and streamflow measurements were made at 15 sites along the Dyje river and its main tributaries the Pulkava, Mlýnská strouha, and Jevišovka (Fig. 3b). The

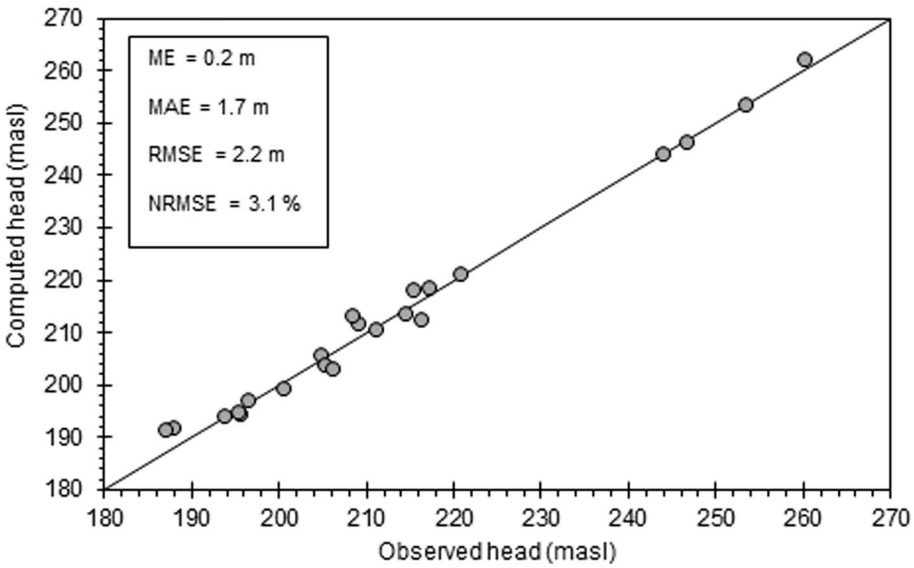

Fig. 6 Calibration plot showing the difference between observed and computed hydraulic heads (masl)

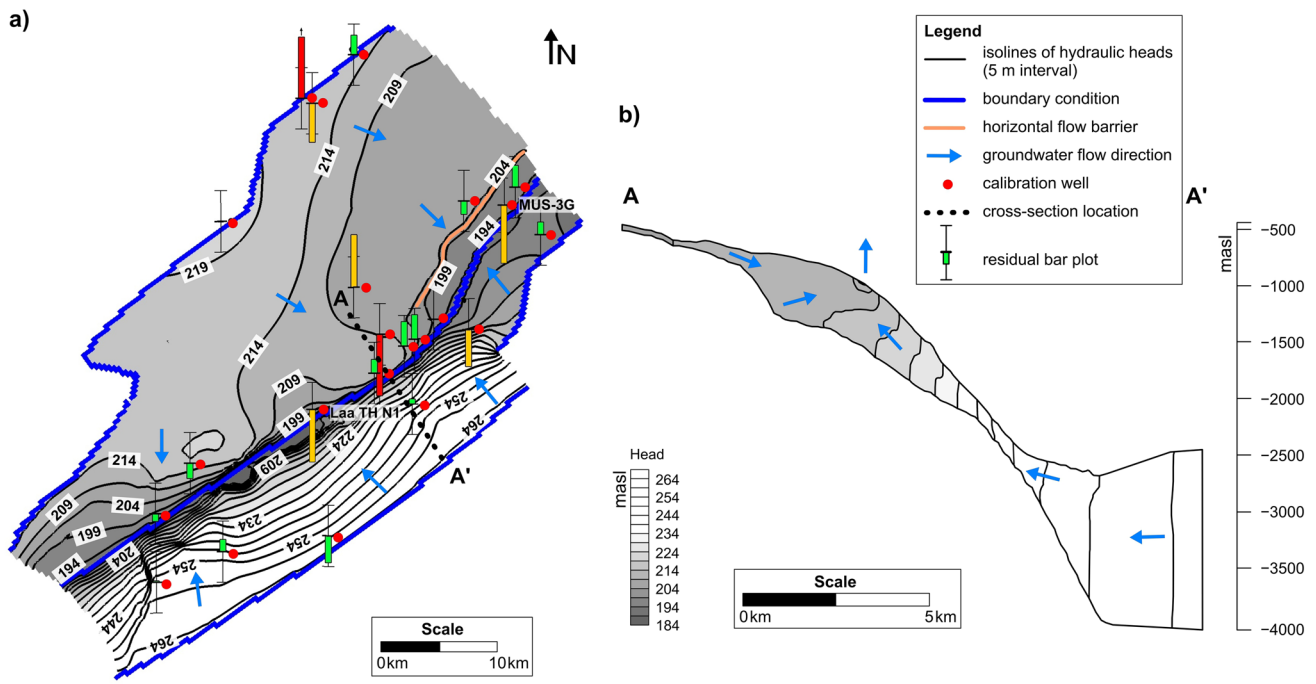

Fig. 7 **a** Spatial distribution of the simulated hydraulic heads at the top layer and **b** the cross-section A-A′ of the modelled aquifer. Coloured bars represent the range of residual error (green < 2 m, yellow > 2 m, red > 4 m)

measurements were taken during low flows when the effect of groundwater influx on the Dyje's chemical composition is more significant. Low streamflows show the value of 3.5 m^3/s observed at site D7. This streamflow corresponds to 35% of the average annual flow rate 9.9 m^3/s (Hydro.chmi.cz 2023). In addition, the chemical composition of groundwater in the Jurassic and overlying Neogene aquifer was evaluated to uncover the origin of groundwater discharged to the Dyje river. The aquifer's hydrochemistry was determined using a chemical analysis of groundwater from 9 wells screened across the Jurassic aquifer (JW1–JW9) and 4 wells (NW1–NW4) screened across the Neogene aquifer. The sampled wells are located along the Jurassic aquifer's discharge zone parallel to the Dyje river (Fig. 3b).

Groundwater chemistry

The Jurassic aquifer samples are characterized by relatively high mineralisation ranging from 2,815 to 26,802 mg/L and Na^+ and Cl^- ion dominance. The Neogene aquifer samples are less mineralised (649–1398 mg/L) exhibiting a range from Ca^{2+} to Na^+ cation and from SO_4^{2-} to Cl^- anion dominance.

Surface water chemistry

Surface water mineralisation ranges from 268 to 1,347 mg/L. A sudden increase in mineralisation from about 300 mg/L at sites D1–D3 to 911 mg/L (D4) was detected in the Dyje river after the discharge of wastewater from the Jungbunzlauer Austria AG factory (Fig. 3b). Wastewater discharge into the Dyje river leads to a marked increase in Na^+, SO_4^{2-} and Cl^- concentrations downstream (Fig. 8a, b). The chemical composition of the Dyje river water is also influenced by its main tributaries the Pulkava, Mlýnská strouha and Jevišovka. The Pulkava stream water chemistry (P1, P2) is characterized by high mineralisation (1258–1347 mg/L) and Mg^{2+} and SO_4^{2-} ion dominance. The stream water sampled from Mlýnská strouha (MS1, MS2) exhibited low mineralisation with a dominance of Ca^{2+} and HCO_3^- ions. The mixture of Mlýnská strouha with Dyje river changes the anion dominance at site D7 from Cl^- to HCO_3^- (Fig. 8c). The Jevišovka stream water (J1, J2) shows medium mineralisation with a dominance of Mg^{2+} and HCO_3^- ions.

Zones of deep groundwater discharge into the Dyje river

Groundwater from the Jurassic aquifer is characterized by high chloride concentrations (1418–15,853 mg/L), significantly exceeding the concentrations in the Neogene aquifer.

The background chloride concentrations in Dyje river are represented by sites D1 (33 mg/L), D2 (35 mg/L) and D3 (34 mg/L). The significant increase in chloride concentrations, from 34 to 172 mg/L in site D4, is due to the wastewater discharge. However, another rise in chloride concentrations was observed in the Dyje river downstream section

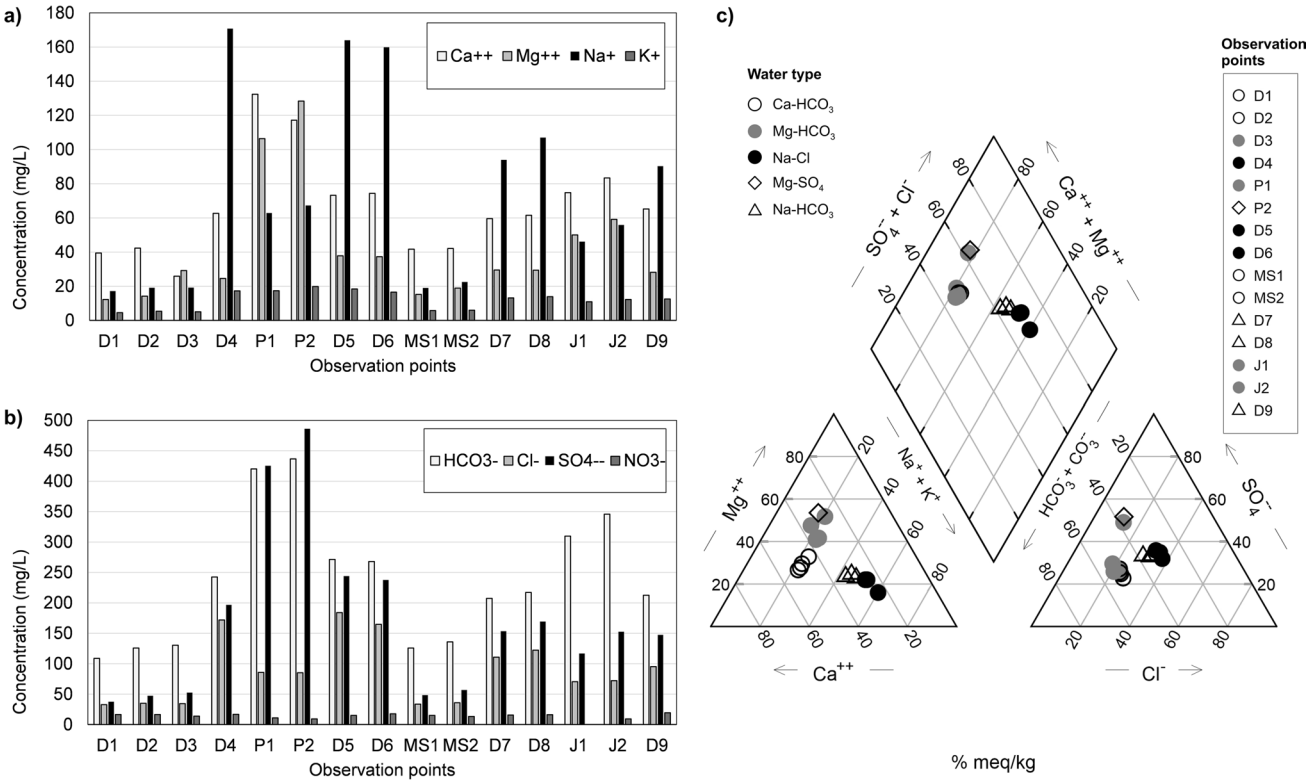

Fig. 8 Spatial variation in **a** cations and **b** anions concentrations at surface water sampling and streamflow measurement (observed) points in Dyje River (D) and its tributaries Pulkava (P), Mlýnská strouha (MS) and Jevišovka (J) and **c** Piper diagram showing the water types

between D4 and D9, where wastewater discharge (2.5 L/s) is negligible (Heis.vuv.cz 2023) and chloride concentrations in the tributaries are low (< 86 mg/L). For a more detailed understanding of the distribution of chloride concentration in the Dyje river, chloride concentrations were calculated at sites designated as P2 + D4, MS2 + D6, J2 + D8, where the main tributaries join the Dyje river, using the analysed concentrations and observed streamflows (Fig. 9). The resulting distribution of chloride concentrations in the Dyje river shows an increase in concentrations in two sections: P2 + D4 to D5 and MS2 + D6 to D8. Given the negligible discharge of wastewater and relatively low chloride concentration in the tributaries, the sections of increasing chloride concentration indicate the discharge of chloride-rich groundwater. The considerable reduction in streamflow rates observed between sites D1 and D3 (Fig. 9) is caused by drainage into irrigation channels. The measured streamflow rates at all 15 observation sites are listed in the Online Appendix 3.

Deep groundwater discharge rate into the Dyje river

The values of streamflow and chloride concentration at the observation sites were used to determine the chloride-rich groundwater discharge rate into the Dyje river. Calculating the discharge rate requires the characteristic value of chloride concentration in groundwater. The highest contribution of groundwater discharge into the Dyje river is expected to come from the Jurassic aquifer due to transmissivity, which is likely to significantly exceed that of the Neogene aquifer. Because of the high variability in chloride concentration along the discharge zone of the Jurassic aquifer (standard deviation of 3,514 mg/L), both mean and median chloride concentration, corresponding to 3,904 and 2,108 mg/L, were taken into account.

The resulting groundwater discharge rate in zone 1 is 26–47 L/s and 16–38 L/s in zone 2 (Fig. 9). The total discharge from the Jurassic aquifer into the observed section of the Dyje river is 42–85 L/s. If only the Neogene aquifer's discharge were considered, the total groundwater discharge would be 768–937 L/s given the mean and median chloride concentrations in the Neogene aquifer, which are 211 and 192 mg/L, respectively. However, the observed streamflow values exclude such high groundwater inflow in both discharge zones (Fig. 9).

The discharge rate into the Dyje river, 85 L/s, as estimated from the median chloride concentration in the Jurassic aquifer, matches the groundwater flux of 80 L/s computed by the numerical model in the discharge zone parallel to the Dyje river.

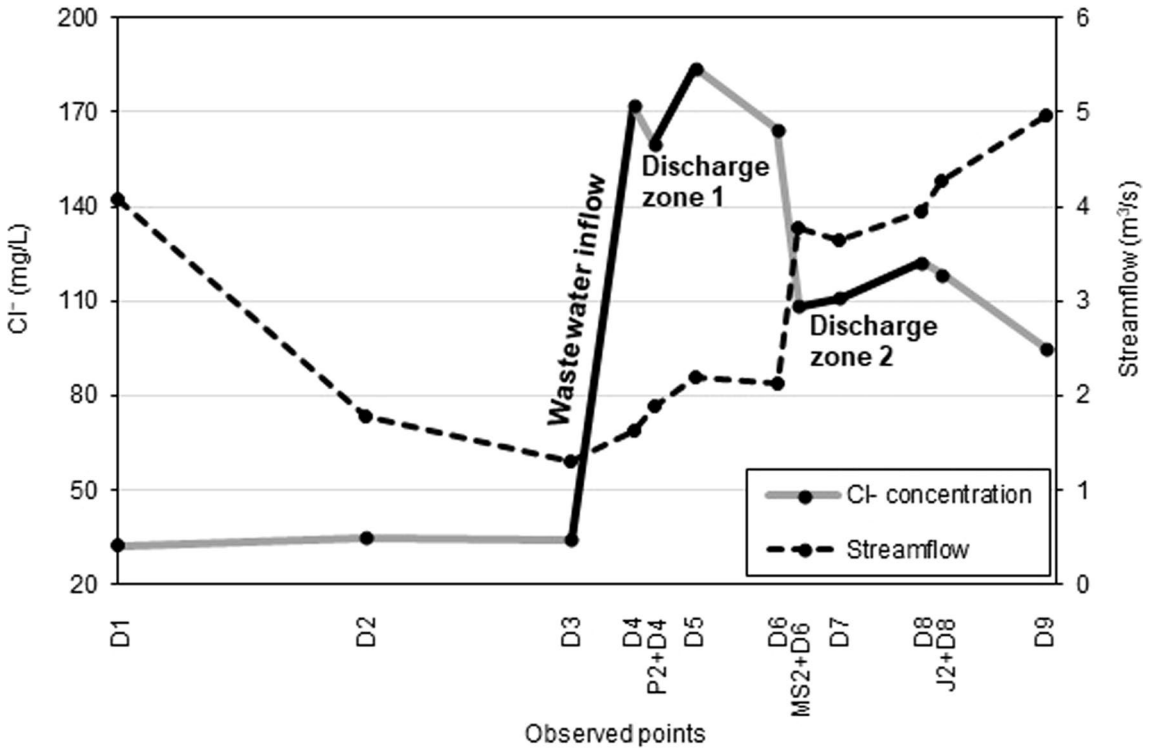

Fig. 9 Spatial variability in chloride concentrations and streamflow rates in the Dyje river

Considering the groundwater discharge of 85 L/s, the Jurassic aquifer discharge supplies about 14 tons of chlorides per day into the Dyje river.

Wastewater inflow to the Dyje River is about 460 L/s (Procházková et al. 2016). Thus, the wastewater chloride concentration, based on concentration and streamflow observed at sites D3 and D4, is approximately 490 mg/L. The wastewater discharge into the Dyje river supplies about 19 tons of chlorides per day. Comparing the chloride mass supplied into river by wastewater and groundwater discharge shows that the Jurassic aquifer discharge is an important contributor to chloride loading of the Dyje river.

Conclusions

This study provides an insight into the groundwater flow in the deep transboundary Jurassic aquifer of a regional scale, reaching depths of up to 3 km below the ground surface. To investigate the groundwater flow pattern of the aquifer, a 3D numerical model of the flow system with variable density and viscosity was developed based on hydrogeological data gathered as part of cross-border cooperation between the Czech Republic and Austria.

The study shows a relatively high groundwater flux of 350 L/s in the modelled part of the Jurassic aquifer. The aquifer discharges into overlying Neogene aquifer along the Mušov Zone, separating the aquifer into relatively shallow northwestern and deeper southeastern part.

The northeastern part of the discharge zone is parallel to the Dyje river, which is the primary drainage system in the region. The simulated groundwater discharge from this part of the aquifer is about 80 L/s. The expected upward groundwater flow from the Jurassic aquifer to the Dyje River was verified by sampling of the river water and streamflow measurements.

The groundwater of the Jurassic aquifer is highly mineralised with a dominance of Na^+ and Cl^- ions. Three river sections of significant increase in chloride concentrations were identified. The highest increase of chloride concentration is caused by wastewater inflow. However, two other sections of increased chloride concentrations were detected in an area without wastewater inflow and with low background chloride concentrations. This indicates that the Jurassic aquifer discharges groundwater into the Dyje river in these sections. The discharge rate of up to 85 L/s, determined by the median chloride concentrations in the Jurassic aquifer and chloride concentrations and streamflow observed in the Dyje river, conforms to the simulated value. This discharge from the Jurassic aquifer to the Dyje river represents a significant natural source of high chloride concentrations, adding about 14 tons of chloride per day. Both wastewater inflow and Jurassic aquifer discharge leads to significant increase in river

mineralisation especially in periods of low streamflow. Such periods become more frequent.

The findings have value for the assessment of the Dyje's water quality and demonstrate that groundwater from deep aquifers can be a significant part of river discharge not influenced by actual climate effects. Furthermore, groundwater from several kilometres depth can be an important source to a river's overall chemical load. This has implications for environmental studies and assessments at least in the Dyje's watershed. The Pasohlávky and Laa an der Thaya spas extract actually only one percent of the calculated groundwater flow and the understanding of the deep southeastern aquifer is vital to the sustainable development of the thermal mineral water spas. Some aspects of the transboundary Jurassic aquifer are still not solved by the numerical modelling. The age of the deep groundwater in the southeast and the origin of the hydraulic gradient for the up-flow are open questions as well as the volume of the highly mineralised groundwater or a possible inflow to this groundwater body.

Supplementary Information The online version contains supplementary material available at https://doi.org/10.1007/s12665-024-11670-7.

Acknowledgements The authors would like to thank to Mag. Magdalena Bottig (Geological Survey of Austria) and Dr. Vladimir Opletal (MND company) for the provision of data and geophysical survey evaluation. We are also very grateful to Mgr. Zdenek Vavricek and Mgr. Petr Vanicek for water physical characterization and help with the field measurements. We would like to thank to the Czech Hydrometeorological Institute as well for providing the data used within this study. For the chemical analyses we would like to thank to Pavel Kadlec from the Department of Geological Sciences, Masaryk University, Brno. We sincerely thank to the editor and reviewers for taking the time to review the manuscript and for their constructive and helpful comments leading to the improvement of this study.

Author contributions All authors contributed to the preparation and final design of the manuscript. The first draft of the manuscript was written by KC and AR and all authors commented on previous versions of manuscript. BP and TK contributed to the final results of the study. JZ contributed to the field data interpretation and together with TRR revised the manuscript critically. All authors reviewed the manuscript carefully and approved the final version to be published.

Funding Open access publishing supported by the National Technical Library in Prague. This study was supported by the cross-border project Interreg HTPO (Hydrothermal potential of the area, ATCZ167).

Data availability The data that support the findings of this study are available from the corresponding author, KC, upon reasonable request.

Declarations

Conflict of interest The authors have no financial or proprietary interests in any material discussed in this article.

References

Adámek J (1974) Hluboký strukturní průzkum oblasti Mušov, etapa II (Deep structural survey of the Mušov area, stage II) (in Czech). MND, Hodonín

Adámek J (1977) Několik poznámek o nových výsledcích v oblasti jižní části karpatské předhlubně (Some notes on new results in the area of the southern part of the Carpathian foredeep) (in Czech). Zem Plyn Nafta 22(1):7–12

Adámek J (1986) Geologické poznatky o stavbě mezozoika v úseku jih jihovýchodních svahů českého masivu (Geological findings on the structure of the Mesozoic in the section of the south-south-eastern slopes of the Czech massif) (in Czech). Zem Plyn Nafta 31(4):453–484

Adámek J (2003) Miocén karpatské předhlubně na jižní Moravě, geologický vývoj a litostratigrafické členění (The Miocene of the Carpathian Foredeep in southern Moravia, geological development and lithostratigraphic classification) (in Czech. Zpr Geol Výzk v Roce 2002 36:9–10

Adámek J (2005) The Jurassic floor of the Bohemian Massif in Moravia—geology and paleogeography. Bull Geosci 80(4):291–305

Adámek J, Balun P, Dostálek J, Guryča I, Jandová B, Karbanová E, Michalíček M, Němcová A, Řehánek J (1990) Geologická část závěrečné zprávy o geotermálním vrtu Mušov-3(G) (Geological part of the final report about the geothermal well Mušov-3(G)) (in Czech). Moravské naftové doly, s. p. odbor průzkumné geologie, Hodonín

Agossou A, Yang JS, Lee JB (2022) Evaluation of potential seawater intrusion in the coastal aquifers system of Benin and Effect of countermeasures considering future sea level rise. Water. https://doi.org/10.3390/w14244001

Beheshti J, Javadi S, Hosseini SA, Moghaddam HK (2022) Evaluation of strategies for pumping optimization of coastal aquifers using numerical simulation and game theory. Environ Earth Sci 81:340. https://doi.org/10.1007/s12665-022-10459-w

Bína J, Demek J (2012) Z nížin do hor: Geomorfologické jednotky České republiky (From lowlands to mountains: Geomorphological units of the Czech Republic) (in Czech). Academia, Praha

Brzobohatý R, Cicha I (1993) Karpatská předhlubeň (Carpathian foredeep). In: Přichystal A, Obstová V, Suk M (ed) Geologie Moravy a Slezska. Sborník příspěvků k 90. výročí narození prof. Dr. Karla Zapletala (Geology of Moravia and Silesia. Proceedings to the 90th birth anniversary of prof. Dr. Karla Zapletala) (in Czech). Moravské zemské muzeum a Sekce geologických věd PřF MU, Brno pp 123–128

Chang SW, Chung IM, Kim MG, Yifru BA (2020) Vulnerability assessment considering impact of future groundwater exploitation on coastal groundwater resources in northeastern Jeju Island, South Korea. Environ Earth Sci 79:498. https://doi.org/10.1007/s12665-020-09254-2

Chlupáč I, Brzobohatý R, Kovanda J, Stráník Z (2002) Geologická minulost České republiky (Geological history of the Czech Republic) (in Czech). Academia, Praha

Chmi.cz (2023) Portál ČHMÚ. Mapy charakteristik klimatu. Dlouhodobý průměr 1991–2020. Průměrná roční teplota vzduchu, roční úhrn srážek. (Portal CHMI. Climate maps. Long-term mean

1991–2020. Annual mean temperature, annual sum of precipitation) (in Czech). https://www.chmi.cz/historicka-data/pocasi/mapy-charakteristik-klimatu. Accessed 4 Oct 2023

Colombani N, Mastrocicco M, Prommer H, Sbarbati C, Petitta M (2015) Fate of arsenic, phosphate and ammonium plumes in a coastal aquifer affected by saltwater intrusion. J Contam Hydrol 179:116–131. https://doi.org/10.1016/j.jconhyd.2015.06.003

Cooper HH, Jacob CE (1946) A generalized graphical method for evaluating formation constants and summarizing well field history. Trans Am Geophys Union 27:526–534. https://doi.org/10.1029/TR027i004p00526

Custodio E (2002) Aquifer overexploitation: what does it mean? Hydrogeol J 10(2):254–277. https://doi.org/10.1007/s10040-002-0188-6

De Louw PGB, Oude Essink GHP, Stuyfzand PJ, van der Zee SEATM (2010) Upward groundwater flow in boils as the dominant mechanism of salinization in deep polders, The Netherlands. J Hydrol 394(3–4):494–506. https://doi.org/10.1016/j.jhydrol.2010.10.009

Doherty JE, Hunt RJ (2010) Approaches to highly parameterized inversion–A guide to using PEST for groundwater-model calibration: U.S. Geological Survey Scientific Investigations Report 2010–5169. U.S. Geological Survey, Reston, Virginia, 59 p

Franzová M (1973) Pasohlávky – hydrogeologická studie (Pasohlávky – hydrogeological study) (in Czech). Geotest, n. p., Brno

Franzová M (1986) Neogenní sedimenty jihozápadní části karpatské předhlubně – hydrogeologická syntéza, I. faze (Neogene sediments of the southwestern part of the Carpathian foredeep – hydrogeological synthesis, phase I.) (in Czech). Geotest, n. p., Brno

Freeze RA, Witherspoon PA (1968) Theoretical analysis of regional groundwater flow: 3. Quantitative Interpretations Water. Resour Res 4(3):581–590. https://doi.org/10.1029/WR004i003p00581

Harbaugh AW, Banta ER, Hill MC, McDonald MG (2000) MODFLOW-2000, the U.S. geological survey modular ground-water flow model - User guide to modularization concepts and the ground-water flow process. USGS Open-File Report 00−92. Reston, VA. https://doi.org/10.3133/OFR200092

Heis.vuv.cz (2023) Map: Water Protection and Management. https://heis.vuv.cz/. Accessed 3 June 2023

Hsieh PA, Freckleton JR (1993) Documentation of a computer program to simulate horizontal-flow barriers using the U.S. Geological Survey's Modular Three-dimensional Finite-difference Groundwater Flow Model. U.S. Geological Survey Open-File Report 92e477, 32 p. http://pubs.er.usgs.gov/publication/ofr92477. Accessed 26 Feb 2024

Hydro.chmi.cz (2023) Evidenční list hlásného profilu č. 364 (Record sheet of reporting profile No. 364) (in Czech). https://hydro.chmi.cz/hppsevlist/download?seq=306976. Accessed 1 June 2023

IGRAC (2021) Transboundary Aquifers of the World [map]. Edition 2021. Scale 1 : 50 000 000. Delft, Netherlands: IGRAC (International Groundwater Resources Assessment Centre)

Kapyrin IV (2021) Assessment of density driven convection effect on the dynamics of contaminant propagation on a deep well radioactive waste injection disposal site. J Comput Appl Math. https://doi.org/10.1016/j.cam.2021.113425

Kocman T (2020) Expertní vyhodnocení režimních měření na vrtu MU3G (Expert evaluation of regime measurements in the MUS3G borehole) (in Czech). KOCMAN envimonitoring, Brno

Krásný J, Kullman E, Vrana, K, Dostál I, Kněžek M, Kouřímová J, Procházková J, Sukovitá D, Šuba J, Trefná E (1987) Vysvětlivky k základní hydrogeologické mapě ČSSR 1 : 200 000. List 34 Znojmo (Explanatory notes to the basic hydrogeological map of the ČSSR 1 : 200 000. Sheet 34 Znojmo) (in Czech). ÚÚG, Praha

Krásný J, Císlerová M, Čurda S, Datel JV, Dvořák J, Grmela A, Hrkal Z, Kříž H, Marszałek H, Šantrůček J, Šilar J (2012) Podzemní vody České republiky: Regionální hydrogeologie prostých a minerálních vod (Groundwater in the Czech Republic: Regional hydrogeology of groundwaters and mineral waters) (in Czech). CGS, Praha

Kyrieleis W, Sichardt W (1930) Grundwasserabsenkung bei Fundierungsarbeiten (Groundwater lowering during foundation work), 2nd edition (in German). Springer, Berlin

Langevin CD, Thorne JrDT, Dausman AM, Sukop MC, Guo W (2008) SEAWAT Version 4: A Computer Program for Simulation of Multi-Species Solute and Heat Transport: U.S. Geological Survey Techniques and Methods Book 6, Chapter A22. U.S. Geological Survey, Reston, Virginia, 39 p

Larsen D, Paul J, Cox R (2021) Geochemical and isotopic evidence for upward flow of saline fluid to the Mississippi River Valley alluvial aquifer, southeastern Arkansas, USA. Hydrogeol J 29:1421–1444. https://doi.org/10.1007/s10040-021-02321-3

Malkovsky VI, Pek AA (2013) Effect of natural advection on stabilization of contaminant plume in natural traps at underground disposal of liquid wastes. Water Resour 40(9):716–722. https://doi.org/10.1134/S0097807813070087

Michalíček M, Petrová V, Repková H (2005) Studie termální a minerální vody jižní a střední Moravy (Study of thermal and mineral water in South and Central Moravia) (in Czech). CGS, Brno

Mlejnková H, Kočková E, Žáková Z (2007) Dlouhodobé hodnocení přeshraniční problematiky znečišťování řeky Dyje vlivem rakouského přítoku Pulkavy (Long-term evaluation of the transboundary problems of Dyje/Thaya River pollution by the Austrian tributary Pulkava/Pulkau). In: Kalinová M (ed.) Sborník prací VÚV T.G.M. (Collection of papers VÚV T.G.M.) (in Czech). VÚV T.G.M., Praha, pp 5–28

Moore PJ, Martin JB, Screaton EJ (2009) Geochemical and statistical evidence of recharge, mixing, and controls on spring discharge in an eogenetic karst aquifer. J Hydrol 376(3–4):443–455. https://doi.org/10.1016/j.jhydrol.2009.07.052

Novotná J, Bartoň J (2011) Struktura termálních vod Mušov–Pasohlávky. Vyhodnocení dat (The structure of the Mušov–Pasohlávky. Data evaluation) (in Czech). Geotest, a. s., Brno

Okuhata BK, El-Kadi AI, Dulai H, Lee J, Wada CA, Bremer LL, Burnett KM, Delevaux JMS, Shuler CK (2022) A density-dependent multi-species model to assess groundwater flow and nutrient transport in the coastal Keauhou aquifer, Hawai'I, USA. Hydrogeol J 30(1):231–250. https://doi.org/10.1007/s10040-021-02407-y

Picha FJ, Stráník Z, Krejčí O (2006) Geology and hydrocarbon resources of the outer western Carpathians and their foreland, Czech Republic. In: Golonka J, Picha FJ (eds) The Carpathians and their foreland: geology and hydrocarbon resources, vol 84. AAPG Memoir, Tulsa, pp 49–175. https://doi.org/10.1306/985607M843067

Post V, Kooi H, Simmons C (2007) Using hydraulic head measurements in variable-density ground water flow analyses. Ground Water 45(6):664–671. https://doi.org/10.1111/j.1745-6584.2007.00339.x

Procházková L, Lošťáková Z, Kosour D, Geriš, R, Jahodová D, Husák V (2016) Souhrnná zpráva o vývoji jakosti povrchových vod v povodí Moravy ve dvouletí 2014–2015 (Summary report on the development of surface water quality in the Morava basin in the two-year period 2014–2015) (in Czech). Povodí Moravy, s. p., Brno

Scanlon BR, Mace RE, Barrett ME, Smith B (2003) Can we simulate regional groundwater flow in karst system using equivalent porous media models? Case study, Barton Springs Edwards aquifer. USA J Hydrol 276:137–158. https://doi.org/10.1016/S0022-1694(03)00064-7

Senger RK (1993) Paleohydrology of variable-density ground-water flow systems in mature sedimentary basins: example of the Palo

Duro basin, Texas, USA. J Hydrol 151(2–4):109–145. https://doi.org/10.1016/0022-1694(93)90232-X

Sophocleous M (2004) Groundwater recharge. In: Silveira L, Wohnlich S, Usunoff EJ (eds) Encyclopedia of life support systems (EOLSS), groundwater, vol 1. Developed under the Auspices of the UNESCO, Eolss Publishers, Oxford, pp 111–126

Thiem G (1906) Hydrologische Methoden (Hydrological methods) (in German). Dissertation, J.M. Gebhardt's Verlag, Leipzig

Tolasz R, Míková, T, Valeriánová A, Voženílek V (2007) Atlas podnebí Česka/Climate atlas of Czechia. CHMI, Praha

Topinka M, Ježek P, Štěpánková K, Michalíček M, Horák J, Remšík A, Strnad M, Glombíček J (1992) Vývoj a aplikace metody využití zdroje geotermální energie (Mušov 3 G) (Development and application of the geothermal energy resource utilization method (Mušov 3 G)) (in Czech). Geologické inženýrství a.s., Brno

Tóth J (2009) Gravitational systems of groundwater flow: theory, evaluation, utilization. Cambridge University Press, Cambridge. https://doi.org/10.1017/CBO9780511576546

Xu Z, Hu BX, Davis H, Cao J (2015) Simulating long term nitrate-N contamination processes in the Woodville Karst Plain using CFPv2 with UMT3D. J Hydrol 524:72–88. https://doi.org/10.1016/j.jhydrol.2015.02.024

Yoon S, Lee S, Zhang J, Zeng L, Kang PK (2023) Inverse estimation of multiple contaminant sources in three-dimensional heterogeneous aquifers with variable-density flows. J Hydrol. https://doi.org/10.1016/j.jhydrol.2022.129041

Zheng C, Wang PP (1999) MT3DMS: A modular three-dimensional multispecies transport model for simulation of advection, dispersion, and chemical reactions of contaminants in groundwater systems; documentation and user's guide. Contract Report SERDP-99–1, U.S. Army Engineer Research and Development Center, Vicksburg, MS.